ORIGINAL RESEARCH PAPER

Study of Adsorption of H_2 and CO_2 on Distorted Structure of MOF-5 Framework; A Comprehensive DFT Study

Mehrzad Arjmandi[1], Majid Peyravi[2,]*, Mahdi Pourafshari Chenar[1], Mohsen Jahanshahi[2], Abolfazl Arjmandi[3]

[1]*Chemical Engineering Department, Faculty of Engineering, Ferdowsi University of Mashhad, Mashhad, Iran*
[2]*Nanotechnology Research Institute, Faculty of Chemical Engineering, Babol Noshirvani University of Technology, Babol, Iran*
[3]*Department of Chemical Engineering, Mazandaran University of Science and Technology, Mazandaran, Iran*

ABSTRACT

To investigate the adsorption property of H_2 and CO_2 on the organic ligand of C-MOF-5 (H_2BDC) and T-MOF-5 (ZnO-doped H_2BDC (ZnO-H_2BDC)), Density functional theory (DFT) method was performed. First, the adsorption of ZnO on H_2BDC resulted in examining binding energies, the charge transfer, density of states, dipole moments and adsorption geometries were investigated. The binding properties have been calculated and investigated theoretically for ZnO-doped H_2BDC in terms of binding energies, band structures, Mulliken charges, and density of states (DOSs). According to obtained results, the H_2BDC was strongly doped with ZnO. H_2 and CO_2 adsorption capacities for ZnO-doped H_2BDC are significantly enhanced while there are low adsorption capacities for H_2BDC. According to results, at least in the organic ligand of the MOF-5, the highest and lowest adsorption of CO_2 (or H_2) is attributed to the T-MOF-5 and C-MOF-5 respectively. Our calculations reveal that ZnO-doped H_2BDC system (T-MOF-5) has much higher adsorption energy and higher net charge transfer value than pristine H_2BDC (C-MOF-5). Also by changing in structure from cubic to tetragonal, the main site for H_2 and CO_2 adsorption was changed.

Keywords: *Adsorption, CO_2, DFT, H_2, MOF-5, ZnO*

INTRODUCTION

In recent years, there has been an increasing interest in adsorption of various molecules [1-6] and developing gas storage systems for various applications such as CO_2 capture or H_2 storage [7-10]. By the same token, the metal-organic framework (MOF) family of materials have attracted particular attention due to their fascinating sorption properties [11-13]. In these materials, inorganic clusters (metals) and organic ligands can be connected to adopt a wide range of different structures, which open the possibility of tuning host-guest interactions in order to explore molecular sieving and adsorption properties unavailable in other materials.

One of the most important MOFs is $Zn_4O_{13}C_{24}H_{12}$ framework called as MOF-5, which was invented in 1999 [14]. This framework has potential applications for H_2 storage, CO_2 capture, and catalysts [15]. The MOF-5 consists of Zn_4O nodes which are linked to terephthalate anions (1,4-BDC = 1,4-benzenedicarboxylate) groups to form a porous material (Fig. 1(a)) [14]. It has been recognized that the MOF-5 occupies either cubic

* Corresponding Author Email: *majidpeyravi@nit.ac.ir*

(C-MOF-5) or tetragonal (T-MOF-5) structure [16-20]. Cubic MOF-5 (with ultra-high BET surface area up to 3400 m^2/g) has widely been synthesized by using a "diffusion" method [14] and tetragonal MOF-5 (with a medium surface area) can be synthesized via "direct mixing" approach [16].

The tetragonal MOF-5 is a distorted cubic MOF-5 [18]. Furthermore, this structure distortion was attributed to the presence of ZnO species extra phase and solvent in the pores [15,18-20]. Zhang and Hang Hu [15], showed that the composition $(Zn_{4.28}O_{12.8}C_{24}H_{11.3})$ of cubic MOF-5 sample is consistent with the stoichiometrical formula of $Zn_4O_{13}C_{24}H_{12}$. In contrast, the composition of the tetragonal MOF-5 sample with the calculated formula of $Zn_4O_{13}C_{24}H_{12.6}(ZnO)_{1.59}(H_2O)_{1.74}$ was very different from the stoichiometrical formula of $Zn_4O_{13}C_{24}H_{12}$, because ZnO and H_2O were present. The presence of H_2O might be due to the adsorption of H_2O when it was exposed to air. The formation of ZnO species is due to the reaction between zinc nitrate and H_2O_2 during the synthesis of tetragonal MOF-5.

In our previous work, we have shown that the T-MOF-5 had a lower surface area, lower porosity, smaller and more uniform pore size, and more ZnO molecule than C-MOF-5 [21]. Also in another work, we have synthesized and characterized the C-MOF-5 and T-MOF-5 as adsorbents for H_2 and CO_2 adsorption [22]. We found that the CO_2 adsorption capacity of C-MOF-5 is greater than that of T-MOF-5 and the H_2 adsorption capacity of C-MOF-5 is less than that of T-MOF-5 (at 298 K and 25 bar). This behavior was attributed to more ZnO units in T-MOF-5 than C-MOF-5.

According to literature, adsorption of small molecules in MOF-5 occurs first in a site near the Zn cluster in the large pores (site A' in Fig. 1(b)) [23-27]. Sarmiento-Perez *et al* [28] introduced a similar site that is present in the smaller pore (site B' in Fig. 1(b)). They showed that the site B' in Fig. 1(b) is the main site for CO_2.

As reported in the literature, calculation of the chemical properties of MOF-5 using a representative fragment (such as an organic ligand) is in good agreement with the experimental results [29-31]. Considering the large size of cells in the MOF-5 structure for a quantum mechanics calculation, the model system should be decreased in size. The size reduction can be achieved by separating the H_2BDC linker. Accordingly, in this paper, we considered the adsorption behavior of CO_2 and H_2 molecules on the surface of C-MOF-5 (H_2BDC as a representative section) and T-MOF-5 (ZnO-H_2BDC as a representative section).

In the current study, we examined the adsorption of H_2 and CO_2 on the surface of H_2BDC and ZnO-H_2BDC (as a representative section of C-MOF-5 and T-MOF-5 nanostructures) using DFT calculations. First, we explored the geometric and electronic properties of H_2BDC surfaces upon decoration of ZnO (ZnO-H_2BDC) by examining binding energies, the charge transfer, density of states, dipole moments and adsorption geometries for the probable position. Then, the relaxed H_2BDC and ZnO-H_2BDC ligands are theoretically investigated for H_2 and CO_2 adsorption. In other words, we investigate in detail, the effect of more ZnO molecule in T-MOF-5 nanostructure than C-MOF-5 nanostructure on H_2 and CO_2 adsorption.
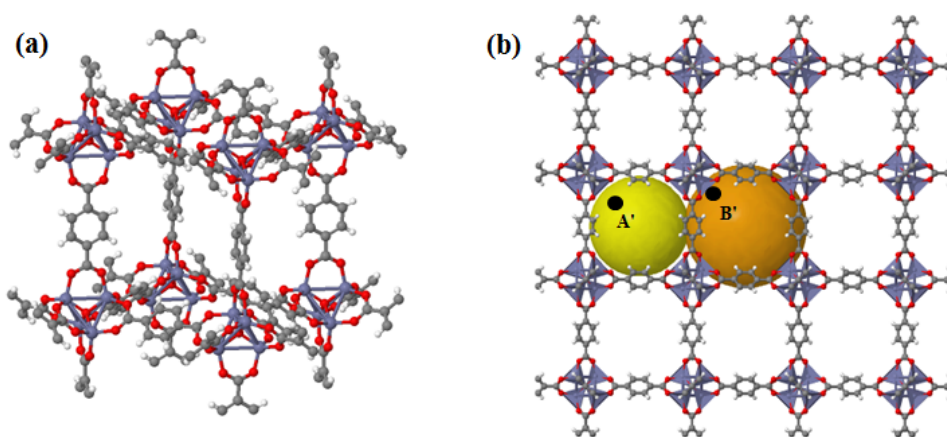

Fig. 1: (a) 1 by 1 by 1 MOF-5 framework, and (b) the small and large pores of MOF-5 framework (denoted as yellow and orange spheres)

J. Water Environ. Nanotechnol., 3(1): 70-80 Winter 2018

71

We have achieved first-principles calculations to walk around the interaction behavior of the H_2 and CO_2 with H_2BDC and ZnO-H_2BDC.

Computational strategy

Geometry optimization, the density of states (DOS), and energy analyses were performed to investigate the adsorption phenomena using Gaussian 09 program package [32] with density functional theory (DFT) at B3LYP/6-31G (d,p) functional/basis set. The 6-31G(d,p) basis set is good for general calculations, besides the B3LYP density functional has been known appropriate for nano-structure studies. The temperature and pressure for all calculations were 298.15 K and 1.0 atm respectively.

A number of possible orientations are considered for H_2BDC, ZnO-H_2BDC, CO_2-H_2BDC, H_2-H_2BDC, CO_2-ZnO-H_2BDC, and H_2-ZnO-H_2BDC, but all input geometries resulted in optimization of limited structures, according to Fig. 2.

The adsorption Energy of ZnO on the H_2BDC is calculated by:

$$E_{ad} = E_{ZnO-H_2BDC} - (E_{H_2BDC} + E_{ZnO}) \qquad (1)$$

where E_{ZnO-H_2BDC} is the energy of H_2BDC interacting with the ZnO and E_{H_2BDC} is the energy of a pristine H_2BDC, and E_{ZnO} is the energy of pristine ZnO. The interaction energy of CO_2 or H_2 (indexed by CO_2/H_2) with pristine H_2BDC and H_2BDC-ZnO are calculated by:

$$E_{ads(H_2BDC)} = E_{CO_2/H_2-H_2BDC} - (E_{H_2BDC} + E_{CO_2/H_2}) \qquad (2)$$

$$E_{ads(ZnO-H_2BDC)} = $$
$$E_{CO_2/H_2-(ZnO-H_2BDC)} - (E_{ZnO-H_2BDC} + E_{CO_2/H_2}) \qquad (3)$$

where $E_{ads(H_2BDC)}$ and $E_{ads(ZnO-H_2BDC)}$ correspond to interaction energy of CO_2/H_2 with H_2BDC and ZnO-H_2BDC, E_{CO_2/H_2-H_2BDC} and $E_{CO_2/H_2-(ZnO-H_2BDC)}$ are energies of H_2BDC and ZnO-H_2BDC interacting with the CO_2/H_2, and E_{CO_2/H_2} is the energy of an isolated CO_2/H_2. All the mentioned energies of the equations are related to equivalently relaxed minimum energy structures. Also chemical potential (μ) [33], hardness (η) [33], softness (S) [33] and electrophilicity (ω) [33] are calculated by:

$$\mu = \frac{(E_{HOMO} + E_{LUMO})}{2} \qquad (4)$$

$$\eta = \frac{(-E_{HOMO} + E_{LUMO})}{2} \qquad (5)$$

$$S = \frac{\eta}{2} \qquad (6)$$

$$\omega = \frac{\mu^2}{2\eta} \qquad (7)$$

where E_{HOMO} and E_{LUMO} are the energies of HOMO and LUMO, respectively.

The charge transferring between CO_2/H_2 and the surface of both H_2BDC and ZnO-H_2BDC is calculated from the varying of the charge concentration on CO_2/H_2 after adsorption and an isolated spice. This calculation has been done by Mullikan charge analysis [34].
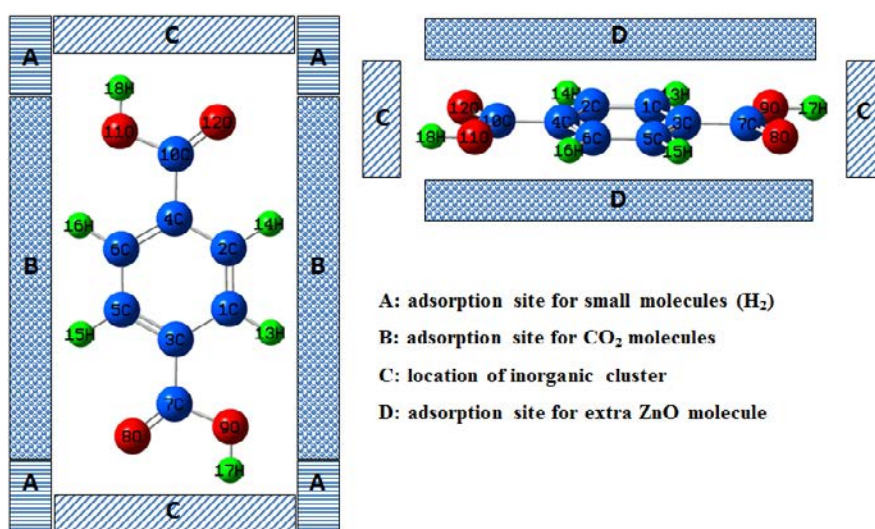

A: adsorption site for small molecules (H_2)
B: adsorption site for CO_2 molecules
C: location of inorganic cluster
D: adsorption site for extra ZnO molecule

Fig. 2: Possible structures for ZnO, CO_2 and H_2 adsorption on top (or down) and side (left or right) sections of ZnO-H_2BDC.

72

J. Water Environ. Nanotechnol., 3(1): 70-80 Winter 2018

RESULTS AND DISCUSSION

Geometries of isolated pristine H_2BDC, ZnO-H_2BDC and their interaction with CO_2 and H_2 have optimized at B3LYP functional at 6-31G(d,p) basis set to allow them to be relaxed. Although the site C in Fig. 2 is the most attractive location for ZnO adsorption, but because this place will be occupied by ZnO molecules, as inorganic cluster, therefore in this study, to investigate the location of extra ZnO adsorption around the H_2BDC, the site A, B, and D in Fig. 2 were investigated. In this paper, we will discuss the strongest adsorption site and use the more stable configurations to further study (for all systems). Fig. 3 shows the optimized unit cell of H_2BDC and ZnO-H_2BDC. The values of adsorption energy, as well as some important

parameters for all relaxed systems, are listed in Table 1. The geometric parameters of H_2BDC are in good agreement with the already reported data [35]. According to results, the location D in Fig. 2 is the best location (in front of location A and B) for ZnO adsorption on H_2BDC (whit high adsorption energy, -111.5627 kJ/mol).

In order to study the adsorption of H_2 and CO_2 on H_2BDC and ZnO-H_2BDC, it is essential to note that there are two possible configurations for CO_2 (O end and C end) to be optimized. In this study, we used the more stable configuration. The interaction of H_2 and CO_2 molecules with H_2BDC and ZnO-H_2BDC on different positions (site A, B, and D in Fig. 2) has been studied using the above-mentioned method and let them be fully optimized.

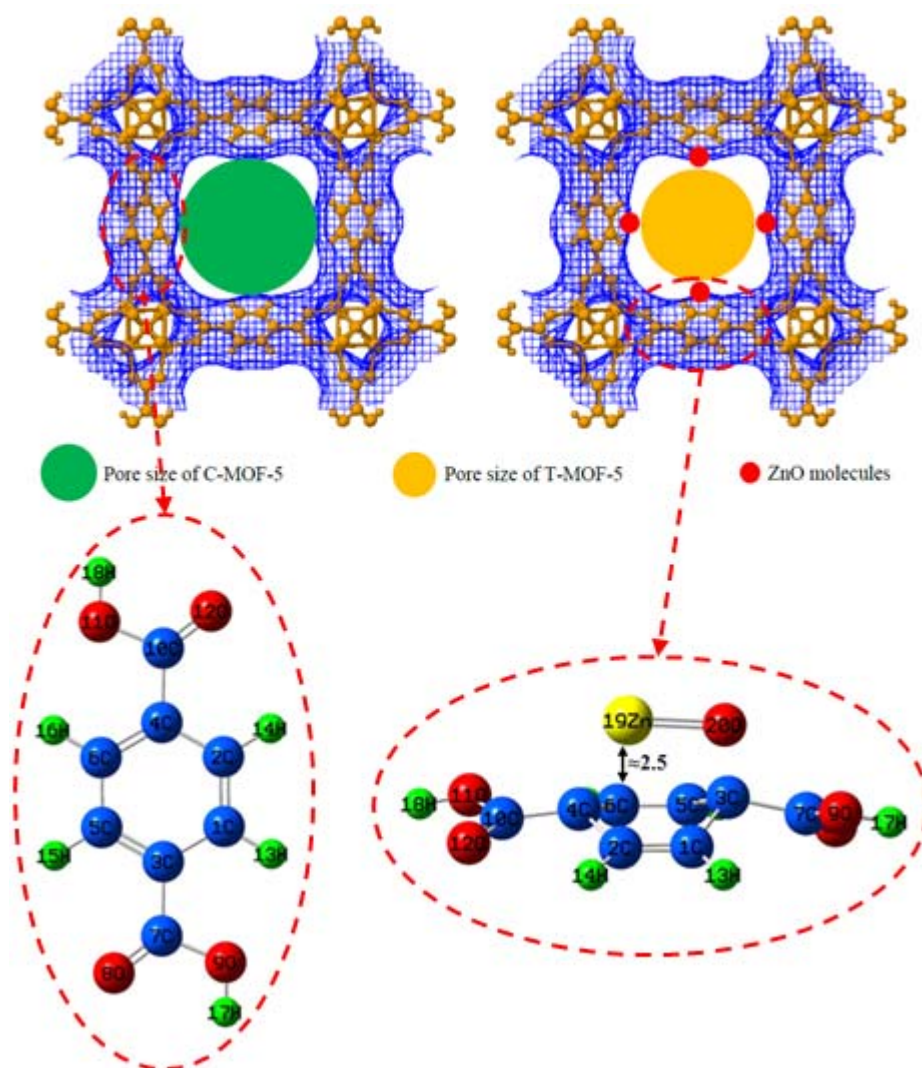Fig. 3: C-MOF-5 and T-MOF-5 frameworks and optimized unit cell of H_2BDC and ZnO-H_2BDC (carbon (blue), oxygen (red), hydrogen (green), zinc (yellow))

J. Water Environ. Nanotechnol., 3(1): 70-80 Winter 2018

73

Fig. 4 shows the optimized unit cell of H_2-H_2BDC and CO_2-H_2BDC in three positions (site A, B, and D in Fig. 2). In this study, we found that there are two main sites for H_2 and CO_2 adsorption (named site A and site B respectively) on H_2BDC, while the E_{ads} for adsorption of H_2 and CO_2 on site D, is very little (as shown in Table 1).

In fact, considering that the organic ligand in MOF-5 is an appropriate representative [29-31], therefore Fig. 4 shows the adsorption behavior of H_2 and CO_2 on C-MOF-5. Accordingly as noted in the previous sections, the T-MOF-5 had more ZnO molecule than C-MOF-5. The differences between two nanocrystal structures bring about the different behavior in gas adsorption. To investigate the adsorption behavior of H_2 and CO_2 on T-MOF-5, the adsorption study on ZnO-H_2BDC (according to Fig. 3 (b)) was done. Fig. 5 shows the optimized unit cell of H_2-ZnO-H_2BDC and CO_2-ZnO-H_2BDC. The H_2 and CO_2 adsorption energies in ZnO-H_2BDC are -7.6125 and -45.6750

kJ/mol, respectively. According to results, we can conclude that, at least in the organic ligand of the MOF-5, the highest and lowest adsorption of H_2 (or CO_2) is attributed to the T-MOF-5 and C-MOF-5 respectively. Also by changing in structure from cubic to tetragonal, the main site for H_2 and CO_2 adsorption was changed. According to obtained results, the interaction of H_2 (or CO_2) on H_2BDC and ZnO-H_2BDC are in the range of physisorption. That's while the interaction between ZnO and H_2BDC is intermediate between chemisorption and physisorption.

Although in this study, the investigations have been done on organic ligand of MOF-5, and according to the overall structure of MOF-5 has not been analyzed, however, the obtained results for H_2 adsorption on H_2BDC and ZnO-H_2BDC (as representative sections of C-MOF-5 and T-MOF-5) are in good agreement with experimental results obtained for H_2 adsorption on C-MOF-5 and T-MOF-5 [22]. Also, the experimental results for
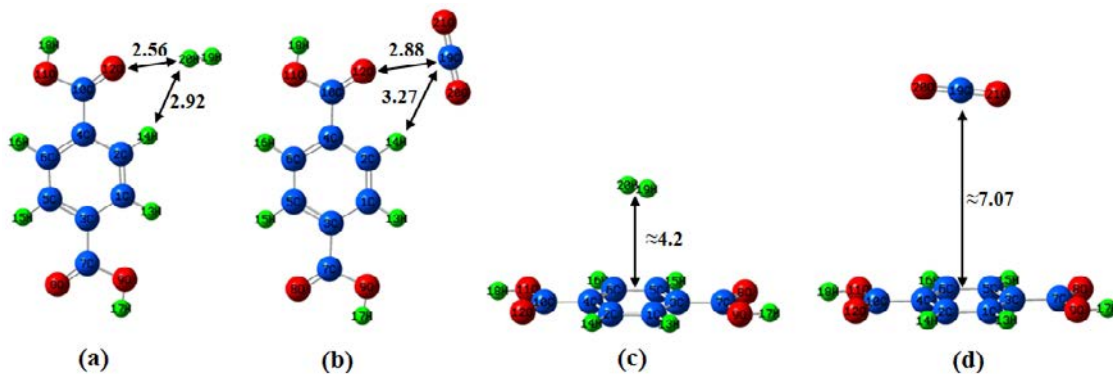

Fig. 4: Relaxed configuration of (a) H_2-H_2BDC-A, (b) CO_2-H_2BDC-B, (c) H_2-H_2BDC-D, (d) CO_2-H_2BDC-D (carbon (blue), oxygen (red), hydrogen (green))
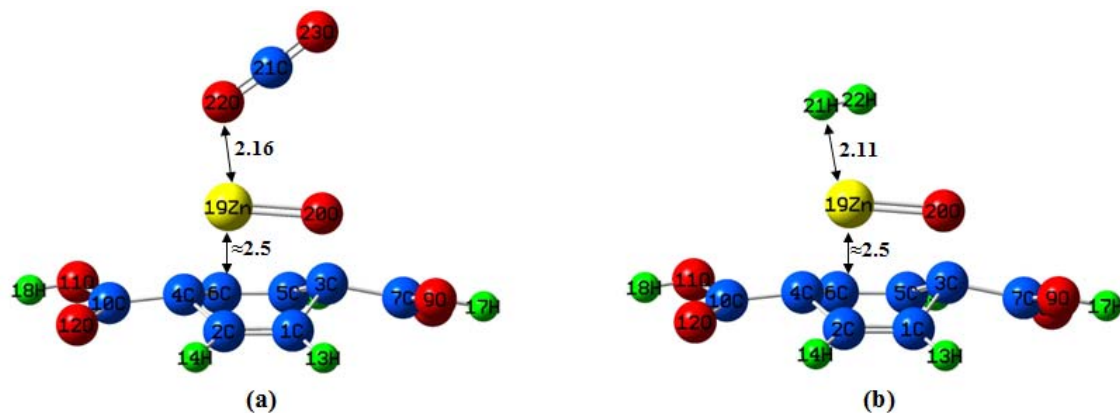

Fig. 5: Optimized unit cell of (a) H_2-ZnO-H_2BDC and (b) CO_2-ZnO-H_2BDC (carbon (blue), oxygen (red), hydrogen (green), zinc (yellow))

74

J. Water Environ. Nanotechnol., 3(1): 70-80 Winter 2018

CO_2 adsorption on C-MOF-5 and T-MOF-5 [22] are in contrast to the obtained results in this study for CO_2 adsorption on H_2BDC and ZnO-H_2BDC (little difference in the same temperature and pressure).

As noted in the previous sections and according to our previous experimental results [21] with changing the structure from cubic to tetragonal, the pore size reduced from 8.67 Å to 6.3 Å. Because the kinetic diameter of hydrogen is very small, then it can be expected that changing the pores size from cubic to tetragonal has little effect on the H_2 diffusivity [19,20] and more effect on the bigger molecules (CO_2 in this study). Also, Sarmiento-Perez *et al* [28] reported that the primary step in the abnormal CO_2 adsorption in MOF-5 is due to synergic and significant contributions from all the three: the inorganic cluster, the organic linker and the 3-D structure of the nanopores. Therefore, the agreement between experimental results [22] and DFT theoretical results presented in this study for H_2 adsorption is attributed to the very small kinetic diameter of H_2. Accordingly, the difference between experimental results (complete structure) [22] and theoretical results presented in this work for CO_2 adsorption, is attributed to the bigger kinetic diameter of CO_2 and high impact of 3-D structure on the adsorption of CO_2. However, this difference does not violate the result of CO_2 adsorption (in this study).

We believe that the adsorption of ZnO on H_2BDC and also the adsorption of H_2 and CO_2 on H_2BDC and ZnO-H_2BDC can be interpreted by the amount of net charge transfer. The amounts of charge transferring between H_2BDC, ZnO, ZnO-H_2BDC, H_2, and CO_2 were simulated at the B3LYP

functional at 6-31G(d,p) basis set. The Mulliken charge analysis is essential analysis for examination the net charge transferring in molecular systems. Table 1 shows the Mulliken charge of interacted ZnO with H_2BDC and also interacted H_2 and CO_2 with H_2BDC and ZnO-H_2BDC. In H_2-H_2BDC-A complex, H_2 detracts about $0.011e^-$ charges to H_2BDC. Reverse transfer of charge achieved in ZnO-H_2BDC, CO_2-H_2BDC-B, CO_2-H_2BDC-D, H_2-H_2BDC-D, CO_2-ZnO-H_2BDC, and H_2-ZnO-H_2BDC complexes whereas ZnO loses about $0.107e^-$ charge from H_2BDC and CO_2 (also ZnO) loses about $0.101e^-$ ($0.059e^-$) charge from ZnO-H_2BDC (also CO_2-H_2BDC) and H_2 (also ZnO) loses about $0.083e^-$ ($0.058e^-$) charge from ZnO-H_2BDC (also H_2-H_2BDC). Also for CO_2-H_2BDC-B and CO_2-H_2BDC-D and H_2-H_2BDC-D complexes no net charge transfer occurs.

As shown in Table 1, significant changes in electronic properties were achieved during adsorption of ZnO on H_2BDC. Also, according to results of Table 1, there are no significant changes in the electronic properties of the pristine H_2BDC surface during interaction with H_2 and CO_2 but significant changes in electronic properties were achieved during adsorption of H_2 and CO_2 on ZnO-H_2BDC.

Supporting confirmation was found in the measured dipole moments (μD) of all systems. The dipole moment is related to the particular property of a molecule which considers data of electronic and geometrical properties [36]. The amounts of the size and structures of the dipole moment for H_2BDC on ZnO-H_2BDC and also for H_2 and CO_2 on the H_2BDC and ZnO-H_2BDC are listed in Table 1. Our computations reveal that when ZnO

Table 1: Calculated charge transfer by Mulliken charge analysis ($Q_{Mulliken}$) on the surface of adsorbents, HOMO energies (E_{HOMO}), LUMO energies (E_{LUMO}), energy of Fermi level (E_{FL}), HOMO/LUMO energy gap (E_g), dipole moment ($μ_D$) and adsorption energy (E_{ads})

System	$Q_{Mulliken}^{CO_2 \text{ or } H_2}$ (e)	$Q_{Mulliken}^{ZnO}$ (e)	E_{HOMO} (eV)	E_{FL} (eV)	E_{LUMO} (eV)	E_g (eV)	$μ_D$ (Debey)	Energy (a.u.)	E_{ads} (kJ/mol)
CO_2	-	-	-10.07	-4.63	0.81	10.88	0.0000	-188.5809	-
H_2	-	-	-11.75	-4.50	2.75	14.50	0.0000	-1.1785	-
ZnO	-	-	-6.63	-5.36	-4.09	2.54	5.0095	-1854.2257	-
Pristine H_2BDC	-	-	-7.38	-4.75	-2.12	5.26	0.0012	-609.4108	-
ZnO-H_2BDC	-	0.107	-6.18	-4.64	-3.10	3.08	2.3339	-2463.6790	-111.5627
CO_2-H_2BDC-B[a]	0.000	-	-7.41	-4.79	-2.18	5.23	0.2563	797.9963	-12.0750
CO_2-H_2BDC-D[a]	0.000	-	-7.40	-4.76	-2.13	5.27	0.0096	-797.9917	≈0.000
CO_2-ZnO-H_2BDC	0.101	0.059	-5.83	-3.92	-2.01	3.82	4.5891	-2652.2773	-45.6750
H_2-H_2BDC-A[a]	-0.011	-	-7.42	-4.79	-2.16	5.26	0.2828	-610.5906	-3.4125
H_2-H_2BDC-D	0.000	-	-7.38	-4.75	-2.12	5.26	0.0034	-610.5893	≈0.000
H_2-ZnO-H_2BDC	0.083	0.058	-6.02	-4.08	-2.14	3.88	3.6621	-2464.8604	-7.6125

[a]Site A, B, and D in Fig. 2

J. Water Environ. Nanotechnol., 3(1): 70-80 Winter 2018

75

comes close to the H_2BDC, the size and directions of μD will change dramatically (from 0.0012 to 2.3339). Also, we found that during H_2 and CO_2 interaction for all systems, the μD is raised. The μD values of the interacted pristine H_2BDC with H_2 (site A), H_2 (site D), CO_2 (site B), and CO_2 (site D) are equal to 0.2828, 0.0096, 0.2563 and 0.0034 Debye, respectively. Also the alteration in the μD of ZnO-H_2BDC upon interaction with mentioned gas compounds increases in the order of CO_2 > H_2. Our results reveal that more dipole moment (4.5891 for CO_2-ZnO-H_2BDC and 3.6621 for H_2-ZnO-H_2BDC) corresponds to more adsorption energy which is in agreement with the results of charge analysis.

To more understand the electronic properties of the organic ligand of C-MOF-5 and T-MOF-5 during adsorption, the density of states (DOS) as the electron density of HOMO-LUMO was calculated for H_2BDC and ZnO-H_2BDC and also their complex was formed with H_2 and CO_2 molecule (see Table 1). Quantum mechanically, the interaction between two reactants takes place because of the interaction of frontier molecular orbitals [37]. HOMO and LOMU have the aptitude to contribute electrons and detract electrons, respectively. However, if a molecule has high HOMO energy, then it will be more unstable and contrariwise because of more reactivity [38,39]. The HOMO and LUMO energy orbitals for H_2BDC and ZnO-H_2BDC are found to be (-7.38 eV, -2.12 eV) and (-6.18 eV, -3.10 eV), respectively. After ZnO doping of H_2BDC (Zn-H_2BDC) and adsorption of H_2 and CO_2 molecule on the surface of H_2BDC and ZnO-H_2BDC, some changes occur in electronic properties.

The HOMO-LUMO energy gap (E_g) is one of the key parameters to recognize the stability as well as the conductivity of resulted adsorptions. Higher E_g results in more stability and less conductivity of resulted complex. The band gaps of the pristine H_2BDC and ZnO-H_2BDC as well as complex forms of CO_2-H_2BDC-B, CO_2-H_2BDC-D, H_2-H_2BDC-A, H_2-H_2BDC-D, H_2-ZnO-H_2BDC CO_2-ZnO-H_2BDC are calculated and are listed in Table 1. Adsorption behaviors of H_2 and CO_2 on H_2BDC and ZnO decorated H_2BDC (ZnO-H_2BDC) are mixed. For pristine H_2BDC, the band gap is almost the same on H_2 and CO_2 adsorption but for ZnO-H_2BDC-H_2 and ZnO-H_2BDC-CO_2 the band gap increases from 3.08 eV (for ZnO-H_2BDC) to 3.88 eV and 3.82 eV, respectively. The calculations revealed the

highest E_g value for interacted ZnO-H_2BDC with H_2 and CO_2, which again correlates well with the high adsorption energies of H_2 and CO_2 on ZnO-H_2BDC compared to H_2BDC.

The change in E_g leads to changes in conductivity. The relationship between conductivity and E_g can be given by [40]:

$$\sigma \propto \exp(-E_g/KT) \tag{8}$$

where σ is the electric conductivity, k is the Boltzmann constant and T is the temperature. According to this equation, a small decrease in E_g leads to significantly higher electrical conductivities. According to results, pristine H_2BDC is not a good adsorbent for H_2 and CO_2 (particularly for H_2) molecule but adsorption of ZnO on H_2BDC significantly enhances its ability towards H_2 and CO_2 adsorption (particularly for CO_2).

Next, we analyzed the densities of states (DOSs) as well as the electron density of HOMO-LUMO to realize how the adsorption of ZnO affects the electronic structure of H_2BDC. Fig. 6 plots the DOSs as well as the electron density of HOMO-LUMO for H_2BDC and ZnO-H_2BDC near the Fermi level (E_F). According to Table 1 and Fig. 5, for pristine H_2BDC, the Fermi level (E_{FL}) is slightly changed from -4.75 eV to -4.79 eV, -4.76 eV, -4.79 eV and -4.75 eV for CO_2-H_2BDC-B, CO_2-H_2BDC-D, H_2-H_2BDC-A, and H_2-H_2BDC-D, respectively. For ZnO-H_2BDC, the E_{FL} is changed a lot from -4.64 eV to -3.92 eV and -4.08 eV for CO_2-ZnO-H_2BDC and H_2-ZnO-H_2BDC, respectively. After comparing the DOS of H_2BDC and ZnO-H_2BDC with that of their interacted forms, we found that the ZnO doping of H_2BDC (ZnO-H_2BDC) causes a significant shift of the occupied orbitals of H_2BDC to high energy levels and observed some change evidence of hybridization in the case of ZnO-H_2BDC systems.

Also according to Fig. 6, The HOMO and LUMO in H_2BDC are uniformly dispersed over the entire skeleton of the pristine organic ligand. The effect of H_2 and CO_2 adsorption on H_2BDC is almost negligible. The decoration of ZnO on H_2BDC brings quite significant changes regarding both energies and densities. Adsorption of ZnO on the surface of H_2BDC increases the energy of HOMO but decreases the energy of LUMO which ultimately results in a decrease in the band gap (from 5.26 to 3.08).

The effect of ZnO doping of H_2BDC (ZnO-H_2BDC) and H_2 and CO_2 adsorption on H_2BDC and ZnO-H_2BDC, and on the electronic structure
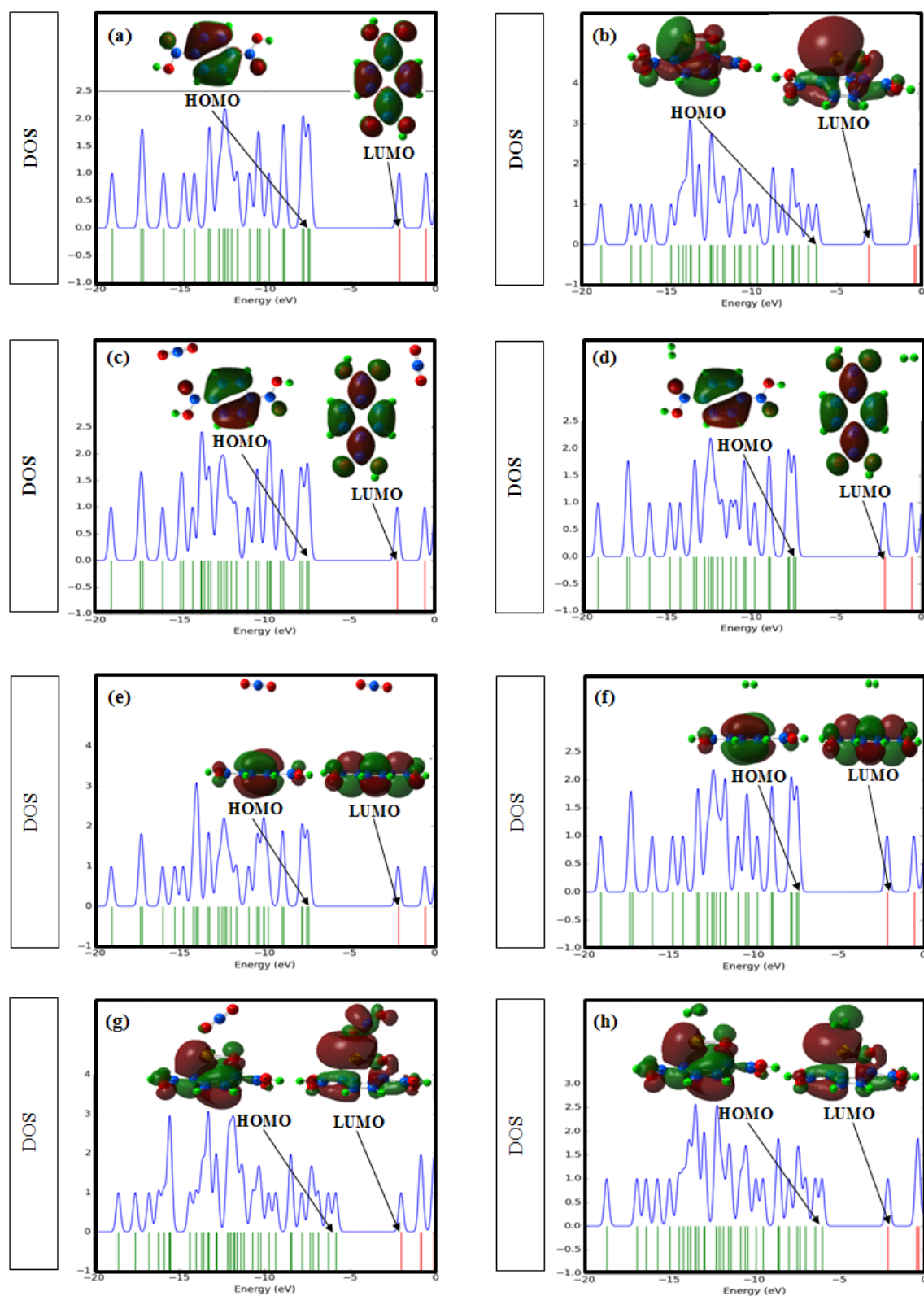
Fig. 6: Electron density of HOMO-LUMO and DOS of (a) pristine H_2BDC, (b) ZnO-H_2BDC, (c) CO_2-H_2BDC-B, (d) H_2-H_2BDC-A, (e) CO_2-H_2BDC-D, (f) H_2-H_2BDC-D, (g) CO_2-ZnO-H_2BDC (h) H_2-ZnO-H_2BDC

J. Water Environ. Nanotechnol., 3(1): 70-80 Winter 2018

77

of the H_2BDC, ZnO-H_2BDC, CO_2-H_2BDC-B, H_2-H_2BDC-A, CO_2-H_2BDC-D, H_2-H_2BDC-D, CO_2-ZnO-H_2BDC, and H_2-ZnO-H_2BDC can be seen in MEP map, shown in Fig. 7. According to Fig. 7(a and b), the pristine H_2BDC has symmetrical potential (due to symmetrical structure) and ZnO atom has positive potential. Also, as shown in Fig. 7(c,d,e and f) the adsorption of H_2 and CO_2 molecules on H_2BDC does not affect on the intensification of positive or negative charge of H_2BDC (particularly for adsorption on-site D Fig. 7(e and f)). For ZnO-H_2BDC, the Zn and O atoms have positive and negative potential (respectively) whereas the atoms in the H_2BDC have almost neutral potential. The negative and positive potential on H_2BDC was changed in ZnO decorated H_2BDC

(ZnO-H_2BDC). Upon adsorption of H_2 and CO_2 (particularly for CO_2) molecule on ZnO-H_2BDC, the negative potential is regenerated on the H_2BDC. The MEP analysis also shows that upon H_2 and CO_2 adsorption, the position of positive potential also shifts to close around of Zn.

We have also calculated the global indices of reactivity for CO_2, H_2, ZnO, H_2BDC, ZnO-H_2BDC, CO_2-H_2BDC-B, CO_2-H_2BDC-D, CO_2-ZnO-H_2BDC, H_2-H_2BDC-A, H_2-H_2BDC-D and H_2-ZnO-H_2BDC systems in order to evaluate how the adsorption of ZnO affects the chemical properties of H_2BDC for H_2 and CO_2 adsorption (Table 2). The energies of LUMO correspond to the electron affinity (define as A) whereas the energies of HOMO can approximately be taken equivalent to ionization potential (define as I)
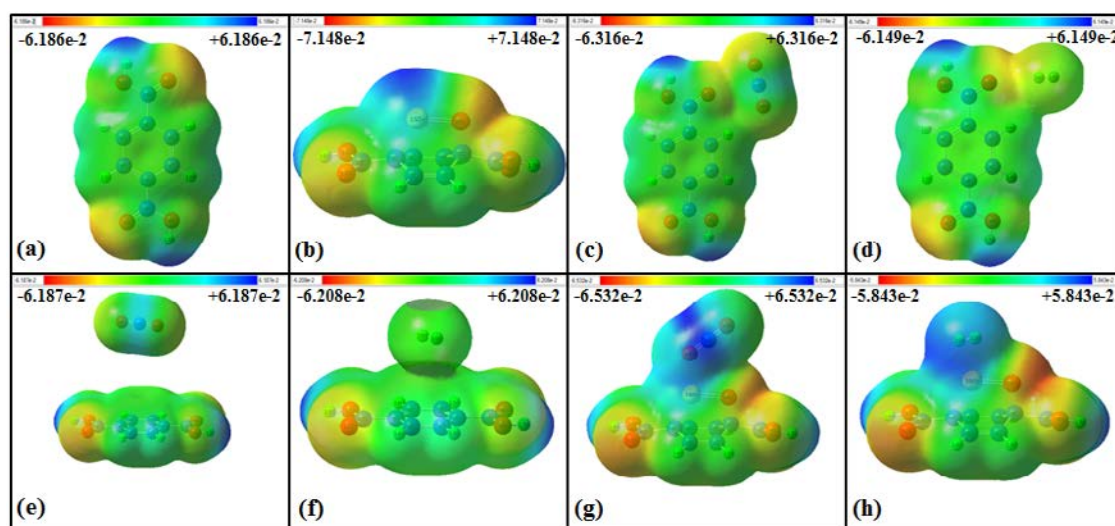

Fig. 7: The MEP of all systems; (a) pristine H_2BDC, (b) ZnO-H_2BDC, (c) CO_2-H_2BDC-B, (d) H_2-H_2BDC-A, (e) CO_2-H_2BDC-D, (f) H_2-H_2BDC-D, (g) CO_2-ZnO-H_2BDC (h) H_2-ZnO-H_2BDC

Table 2: Chemical potential (μ), hardness (η), softness (S) and electrophilicity (ω) of CO_2, H_2, ZnO, H_2BDC, ZnO-H_2BDC, CO_2-H_2BDC-B, CO_2-H_2BDC-D, CO_2-ZnO-H_2BDC, H_2-H_2BDC-A, H_2-H_2BDC-D and H_2-ZnO-H_2BDC systems

System	$I = -E_{HOMO}$ (eV)	$A = -E_{LUMO}$ (eV)	$\eta = (I-A)/2$ (eV)	$\mu = -(I+A)/2$ (eV)	$S = 1/(2\eta)$ (eV^{-1})	$\omega = \mu^2/2\eta$ (eV)
CO_2	10.07	-0.81	5.44	-4.63	0.092	1.970
H_2	11.75	-2.75	7.25	-4.50	0.069	1.397
ZnO	6.63	4.09	1.27	-5.36	0.394	11.311
Pristine H_2BDC	7.38	2.12	2.63	-4.75	0.190	4.289
ZnO-H_2BDC	6.18	3.10	1.54	-4.64	0.325	6.990
CO_2-H_2BDC-B[a]	7.41	2.18	2.61	-4.79	0.192	4.396
CO_2-H_2BDC-D[a]	7.40	2.13	2.63	-4.76	0.190	4.308
CO_2-ZnO-H_2BDC	5.83	2.01	1.91	-3.92	0.262	4.023
H_2-H_2BDC-A[a]	7.42	2.16	2.63	-4.79	0.190	4.362
H_2-H_2BDC-D	7.38	2.12	2.63	-4.75	0.190	4.289
H_2-ZnO-H_2BDC	6.02	2.14	1.94	-4.08	0.258	4.290

[a]Site A, B, and D in Fig. 2

[33]. The ionization potential (I) for pristine H_2BDC is very high and does not decrease upon adsorption of H_2 and CO_2. The decoration of the H_2BDC with ZnO causes a reduction in ionization potential. Also, the ionization potential decreases when H_2 and CO_2 molecules are adsorbed on ZnO decorated H_2BDC. The band gap represents the softness (S) or hardness (η) of a compound. A compound with large band gap is expected to be hard, and conversely. After decoration of the H_2BDC with ZnO, the band gap decreases from 2.63 to 1.54 and it is expected that these complexes (ZnO-H_2BDC) are very soft. According to Table 2, after adsorption of H_2 and CO_2 on H_2BDC the softness values approximately remain unchanged, but after adsorption of H_2 and CO_2 on ZnO-H_2BDC, the softness values declined. The increase in chemical reactivity is electrophilic in nature because the electrophilicity of ZnO-H_2BDC (6.990 eV) is higher than the H_2BDC (4.289 eV).

CONCLUSIONS

We have shown theoretically for the first time that how H_2 and CO_2 adsorption on cubic and tetragonal structure of MOF-5 are different. Accordingly, we optimized the geometries for pristine H_2BDC as well as ZnO doped H_2BDC and their interaction with H_2 and CO_2. Firstly we investigated the possible positions of ZnO on H_2BDC. Among the three sites around H_2BDC (site A, B, and D) for ZnO adsorbed H_2BDC, the site D is more stable than site A and B. According to obtained results, at least in the organic ligand of the MOF-5, the highest and lowest adsorption of CO_2 and H_2 is attributed to the T-MOF-5 and C-MOF-5 respectively. Also among the three sites around H_2BDC (site A, B, and D) by a change in structure from cubic (H_2BDC) to tetragonal (ZnO-H_2BDC), the main site for H_2 and CO_2 adsorption was changed from A and B to D site. Our calculations determine that ZnO-H_2BDC system (as a representative section of T-MOF-5) has much higher adsorption energy, and higher net charge transfer value than pristine H_2BDC (as a representative section of C-MOF-5).

This is a qualitative, exploratory study in which the authors are laying the groundwork for future researches on this subject. It is exploratory because no other researches have been conducted on this specific subject.

CONFLICT OF INTEREST

The authors declare that there are no conflicts of interest regarding the publication of this manuscript.

REFERENCES

1. Abbasi A, Sardroodi JJ, Ebrahimzadeh AR. Chemisorption of CH2O on N-doped TiO2 anatase nanoparticle as modified nanostructure media: A DFT study. Surf Sci. 2016;654(Supplement C):20-32.
2. Abbasi A, Jahanbin Sardroodi J. N-doped TiO2 anatase nanoparticles as a highly sensitive gas sensor for NO2 detection: insights from DFT computations. Environ Sci Nano. 2016;3(5):1153-64.
3. Abbasi A, Jahanbin Sardroodi J. Modified N-doped TiO2 anatase nanoparticle as an ideal O3 gas sensor: Insights from density functional theory calculations. Comput Theor Chem. 2016;1095(Supplement C):15-28.
4. Abbasi A, Sardroodi JJ. A novel strategy for SOx removal by N-doped TiO2/WSe2 nanocomposite as a highly efficient molecule sensor investigated by van der Waals corrected DFT. Comput Theor Chem. 2017;1114(Supplement C):8-19.
5. Abbasi A, Jahanbin Sardroodi J. Van der Waals corrected DFT study on the adsorption behaviors of TiO2 anatase nanoparticles as potential molecule sensor for thiophene detection. Journal of Water and Environmental Nanotechnology. 2017;2(1):52-65.
6. Abbasi A, Jahanbin Sardroodi J, Rastkar Ebrahimzadeh A. TiO2/Gold nanocomposite as an extremely sensitive molecule sensor for NO2 detection: A DFT study. Journal of Water and Environmental Nanotechnology. 2016;1(1):55-62.
7. Marco-Lozar JP, Juan-Juan J, Suárez-García F, Cazorla-Amorós D, Linares-Solano A. MOF-5 and activated carbons as adsorbents for gas storage. Int J Hydrogen Energy. 2012;37(3):2370-81.
8. Saha D, Deng S. Synthesis, characterization and hydrogen adsorption in mixed crystals of MOF-5 and MOF-177. Int J Hydrogen Energy. 2009;34(6):2670-8.
9. Saha D, Wei Z, Deng S. Hydrogen adsorption equilibrium and kinetics in metal–organic framework (MOF-5) synthesized with DEF approach. Sep Purif Technol. 2009;64(3):280-7.
10. Lou W, Yang J, Li L, Li J. Adsorption and separation of CO2 on Fe(II)-MOF-74: Effect of the open metal coordination site. J Solid State Chem. 2014;213(Supplement C):224-8.
11. Wang B, Côté AP, Furukawa H, O'Keeffe M, Yaghi OM. Colossal cages in zeolitic imidazolate frameworks as selective carbon dioxide reservoirs. NATURE. 2008;453:207.
12. Caskey SR, Wong-Foy AG, Matzger AJ. Dramatic Tuning of Carbon Dioxide Uptake via Metal Substitution in a Coordination Polymer with Cylindrical Pores. J Am Chem Soc. 2008;130(33):10870-1.
13. Llewellyn PL, Bourrelly S, Serre C, Vimont A, Daturi M, Hamon L, et al. High Uptakes of CO2 and CH4 in Mesoporous Metal—Organic Frameworks MIL-100 and MIL-101. LANGMUIR. 2008;24(14):7245-50.
14. Li H, Eddaoudi M, O'Keeffe M, Yaghi OM. Design and synthesis of an exceptionally stable and highly porous metal-organic framework. NATURE. 1999;402:276.
15. Zhang L, Hu YH. Structure distortion of Zn4O13C24H12

J. Water Environ. Nanotechnol., 3(1): 70-80 Winter 2018

79

framework (MOF-5). Materials Science and Engineering: B. 2011;176(7):573-8.

16. Huang L, Wang H, Chen J, Wang Z, Sun J, Zhao D, et al. Synthesis, morphology control, and properties of porous metal–organic coordination polymers. Microporous Mesoporous Mater. 2003;58(2):105-14.

17. Kaye SS, Dailly A, Yaghi OM, Long JR. Impact of Preparation and Handling on the Hydrogen Storage Properties of Zn4O(1,4-benzenedicarboxylate)3 (MOF-5). J Am Chem Soc. 2007;129(46):14176-7.

18. Hafizovic J, Bjørgen M, Olsbye U, Dietzel PDC, Bordiga S, Prestipino C, et al. The Inconsistency in Adsorption Properties and Powder XRD Data of MOF-5 Is Rationalized by Framework Interpenetration and the Presence of Organic and Inorganic Species in the Nanocavities. J Am Chem Soc. 2007;129(12):3612-20.

19. Arjmandi M, Pakizeh M. Mixed matrix membranes incorporated with cubic-MOF-5 for improved polyetherimide gas separation membranes: Theory and experiment. J Ind Eng Chem. 2014;20(5):3857-68.

20. Arjmandi M, Pakizeh M, Pirouzram O. The role of tetragonal-metal-organic framework-5 loadings with extra ZnO molecule on the gas separation performance of mixed matrix membrane. Korean J Chem Eng. 2015;32(6):1178-87.

21. Arjmandi M, Pakizeh M. Effects of washing and drying on crystal structure and pore size distribution (PSD) of Zn4O13C24H12 framework (IRMOF-1). Acta Metallurgica Sinica (English Letters). 2013;26(5):597-601.

22. Arjmandi M, Pakizeh M. An Experimental Study of H2 and Co2 Adsorption Behavior of C-MOF-5 and T-MOF-5: A Complementary Study Braz J Chem Eng. 2016;33:225-33.

23. Walton KS, Millward AR, Dubbeldam D, Frost H, Low JJ, Yaghi OM, et al. Understanding Inflections and Steps in Carbon Dioxide Adsorption Isotherms in Metal-Organic Frameworks. J Am Chem Soc. 2008;130(2):406-7.

24. Dubbeldam D, Frost H, Walton KS, Snurr RQ. Molecular simulation of adsorption sites of light gases in the metal-organic framework IRMOF-1. Fluid Phase Equilib. 2007;261(1):152-61.

25. Martin-Calvo A, Garcia-Perez E, Manuel Castillo J, Calero S. Molecular simulations for adsorption and separation of natural gas in IRMOF-1 and Cu-BTC metal-organic frameworks. PCCP. 2008;10(47):7085-91.

26. De Toni M, Pullumbi P, Coudert F-X, Fuchs AH. Understanding the Effect of Confinement on the Liquid–Gas Transition: A Study of Adsorption Isotherms in a Family of Metal–Organic Frameworks. The Journal of Physical Chemistry C. 2010;114(49):21631-7.

27. Fairen-Jimenez D, Seaton NA, Düren T. Unusual Adsorption Behavior on Metal−Organic Frameworks. LANGMUIR. 2010;26(18):14694-9.

28. Sarmiento-Perez RA, Rodriguez-Albelo LM, Gomez A, Autie-Perez M, Lewis DW, Ruiz-Salvador AR. Surprising role of the BDC organic ligand in the adsorption of CO2 by MOF-5. Microporous Mesoporous Mater. 2012;163(Supplement C):186-91.

29. Hu YH, Zhang L. Amorphization of metal-organic framework MOF-5 at unusually low applied pressure. PHYS REV B. 2010;81(17):174103.

30. Yang L-M, Vajeeston P, Ravindran P, Fjellvåg H, Tilset M. Theoretical Investigations on the Chemical Bonding, Electronic Structure, And Optical Properties of the Metal−Organic Framework MOF-5. Inorg Chem. 2010;49(22):10283-90.

31. Petrova T, Michalkova A, Leszczynski J. Adsorption of RDX and TATP on IRMOF-1: an ab initio study. Struct Chem. 2010;21(2):391-404.

32. Frisch M, Trucks G, Schlegel H, Scuseria G, Robb M, Cheeseman J, et al. 09, Revision D. 01, Gaussian. Inc, Wallingford, CT. 2009.

33. Koopmans T. Ordering of wave functions and eigenenergies to the individual electrons of an atom. Physica. 1933;1(1):104-13.

34. Mulliken RS. Electronic Population Analysis on LCAO–MO Molecular Wave Functions. I. The Journal of Chemical Physics. 1955;23(10):1833-40.

35. Lotfi R, Saboohi Y. Effect of metal doping, boron substitution and functional groups on hydrogen adsorption of MOF-5: A DFT-D study. Comput Theor Chem. 2014;1044(Supplement C):36-43.

36. Soltani A, Taghartapeh MR, Mighani H, Pahlevani AA, Mashkoor R. A first-principles study of the SCN− chemisorption on the surface of AlN, AlP, and BP nanotubes. Appl Surf Sci. 2012;259(Supplement C):637-42.

37. Samadizadeh M, Rastegar SF, Peyghan AA. F−, Cl−, Li+ and Na+ adsorption on AlN nanotube surface: A DFT study. Physica E. 2015;69(Supplement C):75-80.

38. Yan M-K, Zheng C, Yin J, An Z-F, Chen R-F, Feng X-M, et al. Theoretical study of organic molecules containing N or S atoms as receptors for Hg(II) fluorescent sensors. Synth Met. 2012;162(7):641-9.

39. Hudson GA, Cheng L, Yu J, Yan Y, Dyer DJ, McCarroll ME, et al. Computational Studies on Response and Binding Selectivity of Fluorescence Sensors. The Journal of Physical Chemistry B. 2010;114(2):870-6.

40. Li SS. Semiconductor physical electronics: Springer Science & Business Media; 2012.

80

J. Water Environ. Nanotechnol., 3(1): 70-80 Winter 2018